2019 18th European Control Conference (ECC)
Napoli, Italy, June 25-28, 2019

LMI Based Robust H2 Control of a Ball Balancing Robot with Omni-wheels

Flávio H. B. Lima[1], Eduardo Poleze[1], Gabriel P. das Neves[1] and Bruno A. Angélico[1]

***Abstract*— Ball Balancing Robots (BBRs) balance themselves on a sphere. With trajectory planning, they could move towards every direction in the horizontal plane. This work gathers construction aspects, modeling and robust $\mathcal{H}_2$ control applied to a BBR built in laboratory. Modeling a BBR is complex because the system is under-actuated and the motors are not aligned to any coordinates system, requiring torques transformations. The robust $\mathcal{H}_2$ control was designed via LMI formulation. Practical results are presented in order to validate de controller.**

I. INTRODUCTION

Self balancing robots represent a class of nonlinear and unstable system widespread in the mechatronics literature. The two-wheeled self-balancing robot is the most classical example, [1], being the Segway its famous commercial version. Other examples of self-balancing robots include the reaction wheel unicycle [2] and, more recently, the unicycle stabilized by gyroscope precession [3].

Ball-Balancing Robots (BBR) or Ballbots are self-balancing robots that balance themselves on a sphere. They usually have a set of rollers that are positioned around the equator of the sphere [4], or a set of equally spaced omni-directional wheels touching the ball and alloying the movement in any direction of the horizontal plane [5]. This last type has a more complicated model, since it is not trivial the relation among torques and velocities of each wheel and the torques and velocities that balance the robot, as described with details in Section III.

These robots can move in any direction of the horizontal plane without changing their orientation. This represents an advantage, especially in environments with little space, when compared to two-wheeled systems, which need to change the orientation in order to change their motion direction, [6], [7].

It is presented a BBR built with omni-wheels and DC motors, as in [8], as well as its modeling and a robust control application. The same BBR was previously considered in [9], but using a simpler controller. In the modeling procedure, it was considered that the vectors of velocities were directly obtained by deriving the position vectors. This is a valid approach around the equilibrium point. A robust $\mathcal{H}_2$ controller with parametric uncertainties was designed using a Linear Matrix Inequality (LMI) approach.

LMI has been considered as a special tool for designing robust control systems [10]. It allows one to design a Lyapunov stable controller and also to consider a performance index, such as minimizing the $\mathcal{H}_\infty$ and/or the $\mathcal{H}_2$ norm, [11], [12]. Another interesting aspect is that it permits designing robust controllers against parametric uncertainties modeled using a polytopic approach [13], [14].

The paper has the following organization: Section II reports the robot construction aspects in detail. Section III presents the system modeling, while Section IV shows the control design. Practical results are presented in Section V and, finally, Section VI points out the main conclusions.

II. ROBOT CONSTRUCTION

The nominal inertial parameters presented in Table I were obtained from a 3D CAD software model.

TABLE I
BBR PHYSICAL PARAMETERS

Parameter	Value
Mass of the ball (m_b)	0.6 [kg]
Ball's moment of inertia (J_b)	5.68×10^{-3} [kg m^2]
Radius of the ball (R_b)	0.118 [m]
Radius of the wheel (R_w)	0.1179 [m]
Mass of the body	2.7579 [Kg]
Body's moment of inertia in x (J_r)	0.03368376 [kg m^2]
Body's moment of inertia in y (J_p)	0.03382657 [kg m^2]
Body's moment of inertia in z (J_w)	0.02249327 [kg m^2]
Wheel's moment of inertia (J_w)	45.879 $\times 10^{-6}$ [kg m^2]
Distance of the center of mass (d)	0.24380132 [m]
Motor torque constant (K_t)	0.3531 [N m/A]
Motor velocity constant (K_e)	1.3465 [V s^2/rad]
Motor armature resistance (R_m)	2.4 [Ω]

The parameters of the three DC motors are also presented in Table I. They were attached with a separation of 120° between them and with an angle $\psi \approx 50^\circ$ to the vertical axis. Each motor has an incremental encoder for measuring its angular position and estimating its angular velocity. The control hardware is a Teensy 3.2 with ARM Cortex-M4 processor. An IMU GY-87 was considered for obtaining the body's angular velocities and positions. The built is presented in Figure 1.

III. SYSTEM MODELING

The procedure considered in this paper is based on the work presented in [2] for a reaction wheel unicycle and was firstly applied to the ball balancing robot in [9]. The body velocity vectors were directly obtained by deriving the position vectors, which for the BBR is a valid approximation in the vicinity of the equilibrium point. Defining θ_x and θ_y as the angles that the ball rotates around x and y axes, respectively, and θ_p, θ_r and θ_w the robot rotation angles

*This work was supported by Fundação de Amparo à Pesquisa do Estado de São Paulo (FAPESP) for the grant 2017/22130-4.

[1] Dept. of Telecommunications and Control Eng. — Escola Politécnica da USP, São Paulo, Brazil flavio.henrique.lima@usp.br, eduardo.poleze@usp.br, gabriel.pereira.neves@usp.br, angelico@lac.usp.br

978-3-907144-00-8 ©2019 EUCA

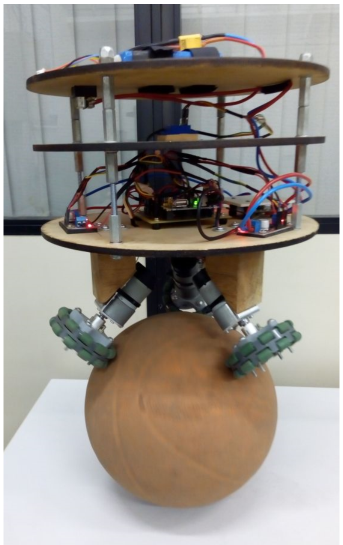

Fig. 1. BBR built in LCA.

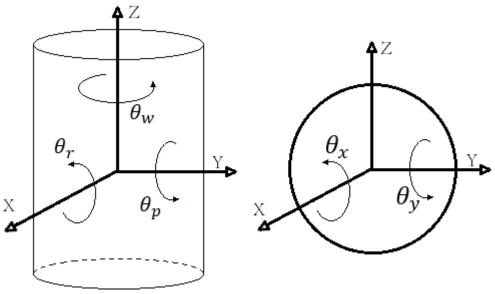

Fig. 2. Angles that describe the motions of the body and the ball.

around y (pitch), x (roll) and z (yaw) axes, respectively, the following vector of generalized variables is defined:

$$q = \begin{bmatrix} \theta_x & \theta_y & \theta_p & \theta_r & \theta_w \end{bmatrix}^\top . \tag{1}$$

All possible motions of the robot can be described by this set of variables, which are represented in the Fig. 2.

It is assumed that the reference frame is fixed on the floor. In relation to this frame, it is possible to describe the position of the center of mass (CoM) of the ball p_b, the CoM of the body, p_c, and the relative position between both CoMs, p_r, as shown in Fig. 3.

Considering R_b the radius of the ball, its position can be expressed by

$$p_b = \begin{bmatrix} R_b\theta_y & R_b\theta_x & R_b \end{bmatrix}^\top . \tag{2}$$

It is assumed that the body is always in touch with the ball, so the distance between the CoM of the ball and the CoM of the body is constant and equal to d. Therefore, it is possible to determine p_r by

$$p_r = \begin{bmatrix} d\sin(\theta_p) \\ -d\cos(\theta_p)\sin(\theta_r) \\ d\cos(\theta_p)\cos(\theta_r) \end{bmatrix} . \tag{3}$$

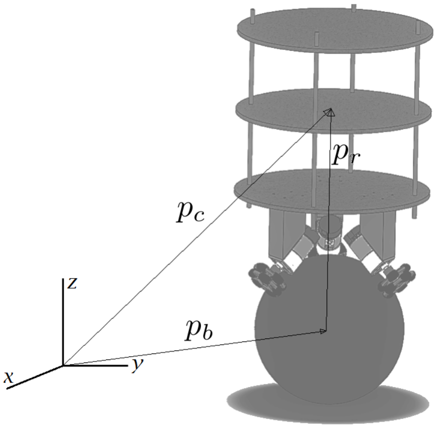

Fig. 3. Robot position described with a single coordinate system.

Hence, the position of the CoM of the body, p_c, is expressed as

$$p_c = p_b + p_r . \tag{4}$$

The linear velocities are directly obtained by deriving the vectors positions, such that

$$v_b = \begin{bmatrix} R_b\dot{\theta}_y & R_b\dot{\theta}_x & 0 \end{bmatrix}^\top , \tag{5}$$

and

$$v_c = \begin{bmatrix} R_b\dot{\theta}_y + d\,\mathrm{c}(\theta_p)\dot{\theta}_p \\ -R_b\dot{\theta}_x - d\,\mathrm{c}(\theta_p)\,\mathrm{c}(\theta_r)\dot{\theta}_r - d\,\mathrm{s}(\theta_p)\,\mathrm{s}(\theta_r)\dot{\theta}_p \\ -d\,\mathrm{c}(\theta_p)\,\mathrm{s}(\theta_r)\dot{\theta}_r - d\,\mathrm{s}(\theta_p)\,\mathrm{c}(\theta_r)\dot{\theta}_p \end{bmatrix} , \tag{6}$$

where $\mathrm{c}(\theta)$ and $\mathrm{s}(\theta)$ represent $\cos(\theta)$ and $\sin(\theta)$, respectively.

The angular velocities of the ball (ω_b) and the body (ω_c) are given by

$$\omega_b = \begin{bmatrix} \dot{\theta}_x & \dot{\theta}_y & 0 \end{bmatrix}^\top \tag{7}$$

and

$$\omega_c = \begin{bmatrix} \dot{\theta}_r & \dot{\theta}_p & \dot{\theta}_w \end{bmatrix}^\top . \tag{8}$$

Being $I_b = \mathrm{diag}(J_b, J_b, J_b)$ the inertia tensor of the ball, its kinetic K_b and potential U_b energies are given by

$$K_b = \frac{1}{2} m_b v_b^T v_b + \frac{1}{2} \omega_b^T I_b \omega_b , \tag{9}$$

and

$$U_b = m_b g R_b . \tag{10}$$

where g stands for the gravitational acceleration.

In the same way, being $I_c = \mathrm{diag}(J_r, J_p, J_w)$ the inertia tensor of the body, its kinetic K_c and potential U_c energies of the body (including the wheels) can be computed as

$$K_c = \frac{1}{2} m_c v_c^T v_c + \frac{1}{2} \omega_c^T I_c \omega_c \tag{11}$$

and

$$U_c = m_c g [R_b + d\cos(\theta_p)\cos(\theta_r)] . \tag{12}$$

Considering J_w the inertia momentum of the omni-wheel around its rotation axis, $\dot{\phi}_i$ the angular velocity of the i-th wheel, the kinetic energy K_w can be computed according to

$$K_w = \sum_{i=1}^{3} \frac{1}{2} \dot{\phi}_i^T J_w \dot{\phi}_i. \tag{13}$$

Assuming that there is no slipping between the omni-wheels and the ball, the velocity of the omni-wheels can be related geometrically to the ball velocities, according to [8]:

$$\dot{\phi}_i = \frac{1}{r_w} (\omega_b \times r_{wi})\, u_{wi}\,, \quad i = 1, 2, 3. \tag{14}$$

where r_{wi} represents the vector from the center of the ball to the point where the i-th wheel is in touch with the ball, u_{wi} is the the versor pointing to the same direction of the linear velocity of the i-th omni-wheel, at the point of contact with the ball, and r_w is the omni-wheels radius.

Hence, the system Lagrangian is computed:

$$L(q, \dot{q}) = \sum K(q, \dot{q}) - \sum U(q), \tag{15}$$

Being $\tau_{\text{ext},i}$ the external torque related to the generalized variable q_i, the Euler-Lagrange equations can be calculated with

$$\frac{d}{dt} \left(\frac{\delta L}{\delta \dot{q}_i} \right) - \frac{\delta L}{\delta q_i} = \tau_{\text{ext},i}. \tag{16}$$

The external torques actuating on the body have the same value and opposite direction to the torques that actuate on the ball. Thus, the external torques can be described by three virtual torques: τ_x, τ_y and τ_z, such that

$$\tau_{\text{ext}} = \begin{bmatrix} -\tau_x & -\tau_y & \tau_y & \tau_x & \tau_z \end{bmatrix}^\top. \tag{17}$$

Let τ_1, τ_2 and τ_3 be the torque of each motor., the relation between virtual motor torques can be written as:

$$\begin{bmatrix} \tau_x \\ \tau_y \\ \tau_z \end{bmatrix} = \begin{bmatrix} \cos(\psi) & \dfrac{-\cos(\psi)}{2} & \dfrac{-\cos(\psi)}{2} \\ 0 & \dfrac{\sqrt{3}\cos(\psi)}{2} & \dfrac{-\sqrt{3}\cos(\psi)}{2} \\ \sin(\psi) & \sin(\psi) & \sin(\psi) \end{bmatrix} \begin{bmatrix} \tau_1 \\ \tau_2 \\ \tau_3 \end{bmatrix}. \tag{18}$$

Being τ_i, PWM_i and $\dot{\phi}_i$ the torque, the duty cycle of the PWM and the velocity related to the i-th motor, respectively, and $V_{\max}$ the maximum input voltage, the motor equation can be described by

$$\tau_i = \frac{K_t (V_{\max} PWM_i - K_e \dot{\phi}_i)}{R_m}. \tag{19}$$

The following state vector is considered:

$$x = \begin{bmatrix} \dot{\theta}_x & \dot{\theta}_y & \theta_p & \dot{\theta}_p & \theta_r & \dot{\theta}_r & \dot{\theta}_w \end{bmatrix}^\top \tag{20}$$

The system inputs are defined as

$$u = \begin{bmatrix} PWM_1 & PWM_2 & PWM_3 \end{bmatrix}^\top. \tag{21}$$

The complete set of nonlinear equations is presented in Appendix VII. The linearized model can be derived as

$$A_{i,j} = \frac{\partial f_i(x,u)}{\partial x_j}, \quad i = 1, ..., 7, j = 1, ..., 7 \tag{22}$$

and

$$B_{i,j} = \frac{\partial f_i(x,u)}{\partial u_k}, \quad i = 1, ..., 7, k = 1, 2, 3, \tag{23}$$

being A and B the state and input matrices, respectively. The system is linearized at the equilibrium point with all states equal to zero, resulting in

$$\dot{x} = Ax + Bu. \tag{24}$$

where, after substituting the numerical values of Table I, it is obtained

$$A = \begin{bmatrix} -13.1706 & 0 & 0 & \dots \\ 0 & -13.1532 & -128.3055 & \dots \\ 0 & 0 & 0 & \dots \\ 0 & 6.2508 & 84.7584 & \dots \\ 0 & 0 & 0 & \dots \\ 6.2623 & 0 & 0 & \dots \\ 0 & 0 & 0 & \dots \end{bmatrix}$$

$$\begin{bmatrix} \dots & 0 & -128.5417 & 0 & 0 \\ \dots & 0 & 0 & 0 & 0 \\ \dots & 1 & 0 & 0 & 0 \\ \dots & 0 & 0 & 0 & 0 \\ \dots & 0 & 0 & 1 & 0 \\ \dots & 0 & 84.9145 & 0 & 0 \\ \dots & 0 & 0 & 0 & 0 \end{bmatrix}, \tag{25}$$

and

$$B = \begin{bmatrix} -39.8656 & 19.9328 & 19.9328 \\ 0 & -34.4790 & 34.4790 \\ 0 & 0 & 0 \\ 0 & 16.3855 & -16.3855 \\ 0 & 0 & 0 \\ 18.9552 & -9.4776 & -9.4776 \\ -30.9915 & -30.9915 & -30.9915 \end{bmatrix}. \tag{26}$$

IV. ROBUST $\mathcal{H}_2$ CONTROLLER VIA LMI

In [15] a robust control with parameter variations is designed for a Ballbot, using Linear Matrix Inequalities. However, the authors considered the model with two rollers positioned around the equator of the ball and one freely spinning wheel, which is quite different from the one with omni-wheel considered in this paper.

Since the BBR is a complex system subject to significant variation in the model caused by small errors in the parameters, the issue of tuning a controller without considering the uncertainties is not trivial. So, a robust $\mathcal{H}_2$ controller via LMI seems to be a good solution.

After some practical tests and analyzing the CAD (3D model), the uncertain parameters were defined as

$$\begin{aligned}
47^{\circ} \leq \quad & \psi & \leq 53^{\circ} \\
0.2408\ [\mathrm{m}] \leq \quad & d & \leq 0.2468\ [\mathrm{m}] \\
0.02863\ [\mathrm{kg\,m^2}] \leq \quad & J_r & \leq 0.03874\ [\mathrm{kg\,m^2}] \\
0.02875\ [\mathrm{kg\,m^2}] \leq \quad & J_p & \leq 0.03890\ [\mathrm{kg\,m^2}] \\
0.01799\ [\mathrm{kg\,m^2}] \leq \quad & J_w & \leq 0.02699\ [\mathrm{kg\,m^2}] \\
2.4812\ [\mathrm{kg}] \leq \quad & M_c & \leq 3.0326\ [\mathrm{kg}] \\
1.4112\ [\mathrm{V\,s/rad}] \leq \quad & K_e & \leq 1.4688\ [\mathrm{V\,s/rad}]
\end{aligned} \tag{27}$$

It can be assumed that the real value is between the maximum and minimum possible, in other words, within the polytope defined by each combination of the parameters $[(A_1, B_1),(A_2, B_2),\ldots,(A_N, B_N)]$. So, the real system is the convex combination of the vertices

$$A(\alpha) = \alpha_1 A_1 + \alpha_2 A_2 + \cdots + \alpha_N A_N, \tag{28}$$

$$B(\alpha) = \alpha_1 B_1 + \alpha_2 B_2 + \cdots + \alpha_N B_N, \tag{29}$$

where

$$\alpha = \begin{bmatrix} \alpha_1 & \alpha_2 & \ldots & \alpha_N \end{bmatrix}, \tag{30}$$

$$\alpha_1 + \alpha_2 + \cdots + \alpha_N = 1. \tag{31}$$

Considering the system in the form

$$\begin{aligned} \dot{x}(t) &= A(\alpha)x(t) + B(\alpha)u(t) + B_w w(t) \\ z(t) &= C_z x(t) + D_z u(t), \end{aligned} \tag{32}$$

where, $A(\alpha)$ and $B(\alpha)$ are the models with the extreme values considered, parameterized in α. Considering a controller K, the closed loop system can be written as

$$\begin{aligned} \dot{x}(t) &= A_{cl}(\alpha)x(t) + B_w w(t) \\ z(t) &= C_{cl}x(t), \end{aligned} \tag{33}$$

where, $A_{cl} = A + BK$ and $C_{cl} = C_z + D_z K$. So, the optimal control $\mathcal{H}_2$, [13], is determinate by

$$\min_{X = X^{\top} > 0} \quad Tr(X) \tag{34}$$

subject to

$$C_{cl}(\alpha)P(\alpha)C_{cl}(\alpha)^{\top} - X < 0, \tag{35}$$

$$A_{cl}(\alpha)P(\alpha) + P(\alpha)A_{cl}(\alpha)^{\top} + B_w B_w^{\top} < 0. \tag{36}$$

As can be seen, the conditions of (35) and (36) are not convex. Hence, it is necessary a convexification procedure. By the Finsler's Lemma, [16], the problem can be rewritten as

$$\min_{X = X^{\top} > 0} \quad Tr(X) \tag{37}$$

subject to

$$\begin{bmatrix} -X & C_z G + D_z Z \\ \star & P(\alpha) - G - G^{\top} \end{bmatrix} < 0, \tag{38}$$

$$\begin{bmatrix} A(\alpha)G + B(\alpha)Z + G^{\top}A(\alpha)^{\top} + Z^{\top}B(\alpha)^{\top} & P(\alpha) - G^{\top} + \xi(A(\alpha)G + B(\alpha)Z) & B_w H(\alpha) \\ \star & -\xi(G + G^{\top}) & 0 \\ \star & \star & I - H(\alpha) - H(\alpha)^{\top} \end{bmatrix} < 0. \tag{39}$$

If a solution to this problem exists, the controller is $K = ZG^{-1}$. It is worth mentioning that with the slack variables, ξ and H, introduced by the Finsler's Lemma, it is possible to obtain a less conservative result.

The matrices C_z, D_z and $B_w = [1\ 1\ 1\ 1\ 1\ 1\ 1]^{\top}$ were chosen to make the controller equivalent to LQR[1], but now considering parametric uncertainties. Hence

$$C_z^{\top} C_z = Q = \mathrm{diag}\begin{bmatrix} 0.0062 & 0.0062 \ldots \\ 32.8281 & 3.6476 & 32.8281 & 3.6476 & 3.6476 \end{bmatrix}, \tag{40}$$

$$D_z^{\top} D_z = R = \mathrm{diag}\begin{bmatrix} 400 & 400 & 400 \end{bmatrix}, \tag{41}$$

$$C_z^{\top} D_z = 0. \tag{42}$$

The ROLMIP software was used [17], which was designed specifically to solve the LMI problems considering uncertain parameter. The resulting controller is given by

$$K = \begin{bmatrix} 0.4419 & 0 & 0 & 0 & \cdots \\ -0.2210 & 0.3827 & 8.5987 & 1.2776 & \cdots \\ -0.2210 & -0.3827 & -8.5987 & -1.2776 & \cdots \\ 9.9269 & 1.4741 & -0.0554 \\ -4.9634 & -0.7371 & -0.0554 \\ -4.9634 & -0.7371 & -0.0554 \end{bmatrix} \tag{43}$$

V. RESULTS

The controller was validated in the real system considering a test with duration of 30 [s]. The results for the angular positions of the body are presented in Fig. 4.

It is possible to observe that the controller was able to keep the angular positions of the body in a range within -5° and 5°, which represents a variation almost imperceptible by eye. In this range, it is valid to consider the linearized model as a good approximation to represent the behavior of the system. In Fig. 5, the results for the angular velocities are presented.

Observing Fig. 5, it can be seen that the body velocities are limited into the range of $-25^{\circ}/s$ to $25^{\circ}/s$. The results for the control efforts, which are the duty cycles of the *PWM*s sent to the actuators, are shown in the Fig. 6. Positive and negative values represent, respectively, motion in counterclockwise and clockwise direction in the actuators axes.

If the initial conditions during the startup are close to the desired state (angular positions and velocities of the body equal to zero), the control efforts do not reach the saturation. During the test, the maximum peak value registered for the PWMs was approximately 70% of the input voltage.

[1] It is similar to choose the weighting matrices Q (states matrix) and R (input matrix).

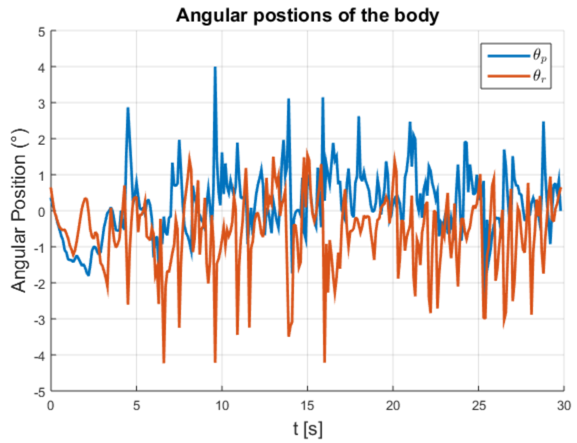

Fig. 4. Results for the angular positions of the body.

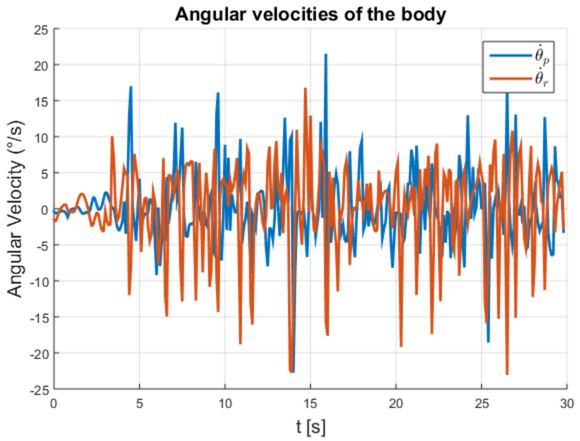

Fig. 5. Results for the angular velocities of the body.

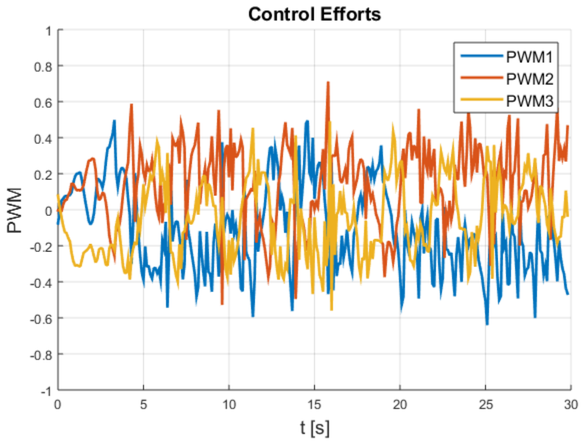

Fig. 6. Results for the control efforts.

VI. Conclusions

A ball balancing robot, which is a non-trivial plant, was built, modeled and controlled. An alternative modeling procedure was considered, based on the absolute position and velocity of each part of the system. The robust $\mathcal{H}_2$ control via LMI, considered parametric errors, was able to stabilize the robot on the ball. During tests, the angles and velocities of the robot were always within a limited range, where the actuators were able to recover the vertical position without reaching saturation. However, in future works, for the system to be able to reject external disturbances and to track a trajectory, stronger actuators are recommended.

Appendix

VII. Complete Nonlinear Model

The nonlinear model can be written as

$$M(q)\ddot{q} + V(q,\dot{q}) + G(q) = Pu, \tag{44}$$

where q is the vector of generalized variables described in (1). The matrix M is given by

$$M(q) = \begin{bmatrix} M_{11} & 0 & 0 & M_{14} & M_{15} & 0 \\ 0 & M_{22} & 0 & M_{24} & 0 & 0 \\ 0 & 0 & M_{33} & 0 & 0 & 0 \\ M_{14} & M_{24} & 0 & M_{44} & 0 & 0 \\ M_{15} & 0 & 0 & 0 & M_{55} & 0 \\ 0 & 0 & 0 & 0 & 0 & M_{66} \end{bmatrix}, \tag{45}$$

with,

$$\begin{aligned} M_{11} &= J_b + M_b R_b^2 + M_c R_b^2, && (46)\\ M_{14} &= -M_c R_b d\,\mathrm{s}(\theta_p)\,\mathrm{s}(\theta_r), && (47)\\ M_{15} &= M_c R_b d\,\mathrm{c}(\theta_p)\,\mathrm{c}(\theta_r), && (48)\\ M_{22} &= J_b + M_b R_b^2 + M_c R_b^2, && (49)\\ M_{24} &= M_c R_b d\,\mathrm{c}(\theta_p), && (50)\\ M_{33} &= J_b, && (51)\\ M_{44} &= M_c d^2 + J_p, && (52)\\ M_{55} &= M_c d^2\,\mathrm{c}(\theta_p)^2 + J_r, && (53)\\ M_{66} &= J_w. && (54) \end{aligned}$$

Matrix V is written as

$$V(q,\dot{q}) = \begin{bmatrix} v_1 & v_2 & v_3 & v_4 & v_5 \end{bmatrix}^\top, \tag{55}$$

where,

$$
\begin{aligned}
v_1 &= (3K_t K_v R_b \dot{\theta}_x \,\mathrm{c}(\psi)^2)/(2R_m R_w) - \dots \\
&\quad M_c R_b d \dot{\theta}_r^2 \,\mathrm{c}(\theta_p)\,\mathrm{s}(\theta_r) - M_c R_b d \dot{\theta}_p^2 \,\mathrm{c}(\theta_p)\,\mathrm{s}(\theta_r) - \dots \\
&\quad 2M_c R_b d \theta_p \theta_r \,\mathrm{c}(\theta_r)\,\mathrm{s}(\theta_p), && (56) \\
v_2 &= (3K_t K_v R_b \dot{\theta}_y \,\mathrm{c}(\psi)^2)/(2R_m R_w) - \dots \\
&\quad M_c R_b d \dot{\theta}_p^2 \,\mathrm{s}(\theta_p), && (57) \\
v_3 &= (3K_t K_v R_b \dot{\theta}_z \,\mathrm{s}(\psi)^2)/(R_m R_w), && (58) \\
v_4 &= -(3K_t K_v R_b \dot{\theta}_w \,\mathrm{c}(\psi)^2 - \dots \\
&\quad M_c R_m R_w d^2 \dot{\theta}_r^2 \,\mathrm{s}(2\theta_p))/(2R_m R_w), && (59) \\
v_5 &= -(3K_t K_v R_b \dot{\theta}_x \,\mathrm{c}(\psi)^2 + 2M_c R_m R_w d^2 \dots \\
&\quad \dot{\theta}_p \dot{\theta}_r \,\mathrm{s}(2\theta_p))/(2R_m R_w), && (60) \\
v_6 &= -(3K_t K_v R_b \dot{\theta}_z \,\mathrm{s}(\psi)^2)/(R_m R_w). && (61)
\end{aligned}
$$

Finally, matrices G and P are described by

$$
G(q) = \begin{bmatrix} 0 \\ 0 \\ 0 \\ -M_c\, d\, g\, \mathrm{c}(\theta_r)\,\mathrm{s}(\theta_p) \\ -M_c\, d\, g\, \mathrm{c}(\theta_p)\,\mathrm{s}(\theta_r) \\ 0 \end{bmatrix}, \qquad (62)
$$

and

$$
P = \begin{bmatrix} -p_{11} & p_{12} & p_{12} \\ 0 & -p_{22} & p_{22} \\ p_{31} & p_{32} & p_{32} \\ 0 & p_{22} & -p_{22} \\ p_{11} & -p_{12} & -p_{12} \\ -p_{31} & -p_{32} & -p_{32} \end{bmatrix}, \qquad (63)
$$

with,

$$
\begin{aligned}
p_{11} &= 12K_t \,\mathrm{c}(\psi)/R_m, && (64) \\
p_{31} &= 12K_t \,\mathrm{s}(\psi)/R_m, && (65) \\
p_{12} &= 6K_t \,\mathrm{c}(\psi)/R_m, && (66) \\
p_{22} &= 6\sqrt{3}K_t \,\mathrm{c}(\psi)/R_m, && (67) \\
p_{32} &= 12K_t \,\mathrm{s}(\psi)/R_m. && (68)
\end{aligned}
$$

ACKNOWLEDGMENT

The authors would like to thank Fundação de Amparo à Pesquisa do Estado de São Paulo (FAPESP) for the grant 2017/22130-4 and Coordenação de Aperfeiçoamento de Pessoal de Nível Superior - Brazil (CAPES) - Finance Code 001.

REFERENCES

[1] S. Kim and S. Kwon, "Nonlinear optimal control design for underactuated two-wheeled inverted pendulum mobile platform," *IEEE/ASME Transactions on Mechatronics*, vol. 22, no. 6, pp. 2803–2808, Dec 2017.

[2] S. I. Han and J. M. Lee, "Balancing and velocity control of a unicycle robot based on the dynamic model," *IEEE Transactions on Industrial Electronics*, vol. 62, no. 1, pp. 405–413, Jan 2015.

[3] H. Jin, T. Wang, F. Yu, Y. Zhu, J. Zhao, and J. Lee, "Unicycle robot stabilized by the effect of gyroscopic precession and its control realization based on centrifugal force compensation," *IEEE/ASME Transactions on Mechatronics*, vol. 21, no. 6, pp. 2737–2745, Dec 2016.

[4] T. B. Lauwers, G. A. Kantor, and R. L. Hollis, "A dynamically stable single-wheeled mobile robot with inverse mouse-ball drive," in *Proceedings 2006 IEEE International Conference on Robotics and Automation (ICRA 2006)*, May 2006, pp. 2884–2889.

[5] M. Kumagai and T. Ochiai, "Development of a robot balancing on a ball," in *2008 International Conference on Control, Automation and Systems*, Oct 2008, pp. 433–438.

[6] U. Nagarajan, A. Mampetta, G. A. Kantor, and R. Hollis, "State transition, balancing, station keeping and yaw control for a dynamically stable single spherical wheel mobile robot," in *Proceedings of the IEEE International Conference on Robotics & Automation (ICRA 2009)*, May 2009, pp. 998 – 1003.

[7] M. Kumagai and T. Ochiai, "Development of a robot balancing on a ball," in *2008 International Conference on Control, Automation and Systems*, Oct 2008, pp. 433–438.

[8] K. van der Blonk, "Modeling and control of a ball-balancing robot," Master's thesis, Internship & Master thesis at ALTEN Mechatronics, Eindhoven, 2014.

[9] L. Flvio H. B., E. Poleze, G. P. d. Neves, and B. A. Anglico, "Ball balancing robot: construction, modeling and control design," in *2018 13th IEEE International Conference on Industry Applications (INDUSCON)*, Nov 2018, pp. 1368–1372.

[10] S. Boyd, L. El Ghaoui, E. Feron, and V. Balakrishnan, *Linear matrix inequalities in system and control theory*. SIAM, 1994, vol. 15.

[11] L. El Ghaoui and S. Niculescu, *Advances in Linear Matrix Inequality Methods in Control*, L. E. Ghaoui and S. lulian Niculescu, Eds. SIAM, 2000.

[12] G. E. Dullerud and F. Paganini, *A Course in Robust Control Theory Book Subtitle — A Convex Approach*, 1st ed., ser. Texts in Applied Mathematics. Springer-Verlag, 1991, vol. 36.

[13] R. C. L. F. Oliveira and P. L. D. Perez, "A convex optimization procedure to compute H2 and hinf norms for uncertain linear systems in polytopic domains," *Optimal Control Applications and Methods*, vol. 29, no. 4, pp. 295–312, 2008. [Online]. Available: http://dx.doi.org/10.1002/oca.825

[14] F. Liao, J. L. Wang, and G.-H. Yang, "Reliable robust flight tracking control: an LMI approach," *IEEE Transactions on Control Systems Technology*, vol. 10, no. 1, pp. 76–89, Aug 2002.

[15] R. A. Garcia-Garcia and M. Arias-Montiel, "Linear controllers for the nxt ballbot with parameter variations using linear matrix inequalities [lecture notes]," *IEEE Control Systems*, vol. 36, no. 3, pp. 121–136, June 2016.

[16] M. C. de Oliveira and R. E. Skelton, *Stability tests for constrained linear systems*, S. R. Moheimani, Ed. London: Springer London, 2001.

[17] C. M. Agulhari, R. C. L. F. de Oliveira, and P. L. D. Peres, "Robust LMI Parser: a computational package to construct LMI conditions for uncertain systems," in *XIX Brazilian Conference on Automation (CBA 2012)*, Campina Grande, PB, Brazil, September 2012, pp. 2298–2305.